Alkyne−Acetylide Coupling in Cluster Compounds Bearing a Triosmium Carbonyl $Os_3(CO)_8$ Fragment and a High Oxidation State $(C_5Me_5)W(O)_2$ Unit

Chin-Wei Shiu,[†] Yun Chi,*[,†] Cathy Chung,[†] Shie-Ming Peng,[‡] and Gene-Hsiang Lee[‡]

Department of Chemistry, National Tsing Hua University, Hsinchu 30043, Republic of China, and Department of Chemistry and Instrumentation Center, National Taiwan University, Taipei 10764, Taiwan, Republic of China

Received January 20, 1998

Treatment of acetylide cluster $Cp^*WOs_3(\mu\text{-}O)_2(\mu\text{-}CCPh)(CO)_9$ (**1**), $Cp^* = C_5Me_5$, with diphenylacetylene affords two cluster complexes $Cp^*W(O)Os_3(\mu\text{-}O)(CCPh)(PhC_2Ph)(CO)_8$ (**2**) and $Cp^*W(O)Os_3(\mu\text{-}O)(CCPhCPhCPh)(CO)_8$ (**3a**) by alkyne coordination and cluster-assisted formation of C−C bonds between acetylide and alkyne, respectively. For the reaction with phenylacetylene, only the coupled product $Cp^*W(O)Os_3(\mu\text{-}O)(CCPhCHCPh)(CO)_8$ (**3b**) is obtained, together with a small amount of $Cp^*W(O)Os_3(\mu\text{-}O)(CCPhCCHPh)(CO)_8$ (**4**). Complex **2** slowly converts to **3a** and the complex $Cp^*W(O)(\mu\text{-}O)Os_3(CCPhCPhCPh)(CO)_8$ (**5a**) when heated in toluene, whereas the formation of **4** is believed to pass through a pathway involving an alkyne-to-vinylidene rearrangement. The conversion from complexes **3** to **5** demonstrates a unique skeletal isomerization involving the interchange of a $Cp^*W(O)_2$ unit and one $Os(CO)_3$ fragment.

Introduction

In recent years a great deal of research has been focused on studying mixed-metal cluster complexes of group 8 metal atoms, such as osmium and ruthenium. In particular, it is the observed changes in both the structures and reactivity patterns, relative to the homonuclear analogues, that have stimulated interest in this class of cluster complexes.[1] Our experience in the synthesis of these heterometallic clusters prompted us to investigate new heterometallic systems in which the transition-metal atoms are in the highly disparate oxidation states and coordination environment. Thus, we have synthesized a series of oxo−carbonyl cluster compounds, which contain an oxo or a dioxo metal fragment coordinated to the metal carbonyl unit, by direct oxidation of carbonyl precursor clusters[2] or through cluster building reactions employing the dioxo acetylide complex $Cp^*W(O)_2(CCPh)$ as one of the building blocks.[3] It was anticipated that the incorporation of oxo ligands into these clusters would result in enhanced reactivity or other interesting changes to their molecular structures.

Scheme 1

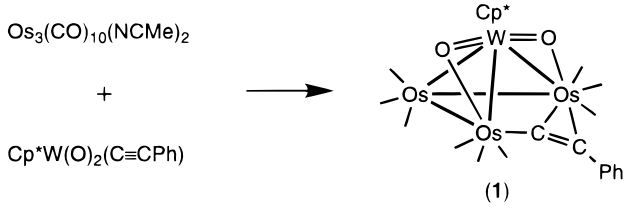

In this paper, we describe the addition of alkynes to a target cluster $Cp^*WOs_3(\mu\text{-}O)_2(CCPh)(CO)_9$, $Cp^* = C_5Me_5$, prepared from addition of $Cp^*W(O)_2(CCPh)$ to $Os_3(CO)_{10}(NCMe)_2$ (Scheme 1)[4] and the subsequent C−C bond formation between ligated acetylide and alkyne in its coordination sphere. An additional feature of this chemistry is a facile change in the bonding capability of the $Cp^*W(O)_2$ fragment which occurs during the transformation. These changes may have implications for the types of interactions which occur between highly reduced platinum metals and oxide supports.[5]

Experimental Section

General Information and Materials. Infrared spectra were recorded on a Perkin-Elmer 2000 FT-IR spectrometer.

[†] National Tsing Hua University.
[‡] National Taiwan University.

(1) (a) Park, J. T.; Shapley, J. R.; Churchill, M. R.; Bueno, C. *Inorg. Chem*. **1983**, *22*, 1579. (b) Shapley, J. R.; Park, J.-T.; Churchill, M. R.; Ziller, J. W.; Beanan, L. R. *J. Am. Chem. Soc.* **1984**, *106*, 1144. (c) Chi, Y.; Shapley, J. R. *Organometallics* **1985**, *4*, 1900. (d) Adams, R. D.; Babin, J. E.; Tasi, M. *Angew. Chem., Int. Ed. Engl.* **1987**, *26*, 685. (e) Park, J. T.; Shapley, J. R.; Bueno, C.; Ziller, J. W.; Churchill, M. R. *Organometallics* **1988**, *7*, 2307. (f) Adams, R. D.; Alexander, M. S.; Arafa, I.; Wu, W. *Inorg. Chem*. **1991**, *30*, 4717. (g) Adams, R. D.; Li, Z.; Lii, J.-C.; Wu, W. *Organometallics* **1992**, *11*, 4001. (h) Adams, R. D.; Barnard, T. S.; Li, Z.; Wu, W.; Yamamoto, J. *Organometallics* **1994**, *13*, 2357. (i) Adatia, T.; Curtis, H.; Johnson, B. F. G.; Lewis, J.; McPartlin, M.; Morris, J. *J. Chem. Soc., Dalton Trans*. **1994**, 1109. (j) Davies, J. E.; Nahar, S.; Raithby, P. R.; Shields, G. P. *J. Chem. Soc., Dalton Trans.* **1997**, 13.

(2) (a) Chi, Y.; Hwang, L.-S.; Lee, G.-H.; Peng, S.-M. *J. Chem. Soc., Chem. Commun*. **1988**, 1456. (b) Chi, Y.; Cheng, P.-S.; Wu, H.-L.; Hwang, D.-K.; Peng, S.-M.; Lee, G.-H. *J. Chem. Soc., Chem Commun*. **1994**, 1839.

(3) (a) Blenkiron, P.; Carty, A. J.; Peng, S.-M.; Lee, G.-H.; Su, C.-J.; Shiu, C.-W.; Chi, Y. *Organometallics* **1997**, *16*, 519. (b) Chao, W.-J.; Chi, Y.; Chung, C.; Carty, A. J.; Delgado, E.; Peng, S.-M.; Lee, G.-H. *J. Organomet. Chem*. **1998**, in press.

(4) Shiu, C.-W.; Chi, Y.; Carty, A. J.; Peng, S.-M.; Lee, G.-H. *Organometallics* **1997**, *16*, 5368.

S0276-7333(98)00025-9 CCC: $15.00
Publication on Web 06/10/1998

^{1}H and ^{13}C NMR spectra were recorded on a Bruker AM-400 (400.13 MHz) or a Bruker AMX-300 (300.6 MHz) instrument. Mass spectra were obtained on a JEOL-HX110 instrument operating in fast atom bombardment mode (FAB). The Cp*W(O)$_2$(CCPh) dioxo acetylide complex was prepared using a published procedure.[6] All reactions were performed under a nitrogen atmosphere using solvents dried with an appropriate reagent. Reactions were monitored by analytical thin-layer chromatography (5735 Kieselgel 60 F_{254}, E. Merck), and products were separated on commercially available preparative thin-layer chromatographic plates (Kieselgel 60 F_{254}, E. Merck). Elemental analyses were performed at the NSC Regional Instrumentation Center at National Cheng Kung University, Tainan, Taiwan.

Reaction of 1 with Diphenylacetylene. A toluene solution (60 mL) of Cp*WOs$_3$(μ-O)$_2$(CCPh)(CO)$_9$ (**1**, 124 mg, 0.097 mmol) and diphenylacetylene (88 mg, 0.50 mmol) was heated at 100 °C for 8 h, during which time the color of the solution changed from orange to red. The solvent was removed *in vacuo*, and the residue was taken up in minimum amount of CH_2Cl_2 and separated by thin-layer chromatography. Development with a 1:1 mixture of CH_2Cl_2 and hexane produced two bands, which were extracted from silica gel to yield 108 mg of red Cp*W(O)Os$_3$(μ-O)(CCPh)(PhC$_2$Ph)(CO)$_8$ (**2**, 0.076 mmol, 78%) and 24 mg of red Cp*W(O)Os$_3$(μ-O)(CCPhCPhCPh)(CO)$_8$ (**3a**, 0.017 mmol, 17%) in the order of elution. Crystals of complexes **2** and **3a** suitable for X-ray diffraction study were obtained by recrystallization from CH_2Cl_2 and hexane at room temperature.

Spectral data for **2**: MS (FAB, ^{184}W, ^{192}Os) *m*/*z* 1430 (M$^+$); IR (C_6H_{12}) ν(CO) 2085 (s), 2061 (vs), 2015 (vs), 2005 (sh), 1991 (m), 1978 (vw), 1972 (w), 1942 (m) cm^{-1}; ^{1}H NMR (300 MHz, $CDCl_3$, 297 K) δ 7.58−7.29 (m, 4H), 7.27 (t, 1H, J_{HH} = 6.9 Hz), 6.89−6.74 (m, 8H), 6.47 (d, 2H, J_{HH} = 7.4 Hz), 2.01 (s, 15H); ^{13}C NMR (75 MHz, $CDCl_3$, 253 K) CO δ 181.3, 179.7, 179.4, 178.4, 175.1, 174.2, 173.1, 172.0. Anal. Calcd for $C_{40}H_{30}O_{10}Os_3W$: C, 33.71; H, 2.12. Found: C, 33.54; H, 2.17.

Spectral data for **3a**: MS (FAB, ^{184}W, ^{192}Os) *m*/*z* 1430 (M$^+$); IR (C_6H_{12}) ν(CO) 2082 (s), 2047 (vs), 2002 (vs), 1984 (s), 1952 (w), 1937 (m) cm^{-1}; ^{1}H NMR (300 MHz, $CDCl_3$, 297 K) δ 7.28 (br, 2H), 7.07−6.86 (m, 13H), 1.93 (s, 15H); ^{13}C NMR (75 MHz, $CDCl_3$, 297 K) CO δ 190.5 181.2, 180.1, 180.0, 177.5, 177.4, 176.5, 171.0. Anal. Calcd for $C_{40}H_{30}O_{10}Os_3W$: C, 33.71; H, 2.12. Found: C, 32.92; H, 2.20.

Reaction of 1 with Phenylacetylene. A toluene solution (40 mL) of Cp*WOs$_3$(μ-O)$_2$(CCPh)(CO)$_9$ (**1**, 125 mg, 0.098 mmol) and phenylacetylene (100 μL, 0.98 mmol) was heated at 90 °C for 2 h, during which time the color of the solution changed from orange to red. After removal of the solvent *in vacuo*, the residue was taken up in CH_2Cl_2 and separated by thin-layer chromatography. Development with a 1:1 mixture of CH_2Cl_2 and hexane produced two bands, which were extracted from silica gel to yield 16 mg of red Cp*W(O)Os$_3$(μ-O)(CCPhCCHPh)(CO)$_8$ (**4**, 0.012 mmol, 12%) and 53 mg of red Cp*W(O)Os$_3$(μ-O)(CCPhCHCPh)(CO)$_8$ (**3b**, 0.039 mmol, 40%) in the order of elution. Single crystals of **3b** and **4** were recrystallized from a mixture of CH_2Cl_2 and methanol and of CH_2Cl_2 and hexane, respectively.

Spectral data for **3b**: MS (FAB, ^{184}W, ^{192}Os) *m*/*z* 1354 (M$^+$); IR (C_6H_{12}) ν(CO) 2080 (s), 2047 (vs), 2003 (vs), 1982 (s), 1958 (w), 1942 (m) cm^{-1}; ^{1}H NMR (300 MHz, $CDCl_3$, 297 K) δ 7.73 (d, J_{HH} = 7.6 Hz, 2H), 7.42−7.24 (m, 8H), 7.16 (s, 1H), 1.95 (s, 15H); ^{13}C NMR (75 MHz, $CDCl_3$, 297 K) CO δ 190.0 (br), 182.7 (br), 180.1 (br), 179.0, 178.9, 178.2, 177.0, 171.7; δ 182.1, 151.7 (J_{WC} = 144 Hz), 149.6 (*i*-C_6H_5), 141.5, 139.4 (*i*-C_6H_5), 130.7 (2C, *m*-C_6H_5), 128.5 (*p*-C_6H_5), 128.4 (3C, *o*-C_6H_5 and *p*-C_6H_5), 127.8 (2C, *o*-C_6H_5), 127.6 (2C, *m*-C_6H_5), 120.6 (C_5Me_5), 107.8 (*C*H), 11.4 (C_5Me_5). Anal. Calcd for $C_{34}H_{26}O_{10}Os_3W$: C, 30.27; H, 1.94. Found: C, 30.15; H, 1.99.

Spectral data for **4**: MS (FAB, ^{184}W, ^{192}Os) *m*/*z* 1354 (M$^+$); IR (C_6H_{12}) ν(CO) 2079 (s), 2043 (vs), 2019 (vs), 2002 (vs), 1994 (s), 1981 (s), 1965 (m), 1949 (m) cm^{-1}; ^{1}H NMR (300 MHz, $CDCl_3$, 297 K) δ 7.55 (d, 2H, J_{H-H} = 7.6 Hz), 7.40−7.23 (m, 7H), 7.17 (t, 1H, J_{HH} = 7.3 Hz), 6.89 (s, 1H), 2.24 (s, 15H); ^{13}C NMR (75 MHz, $CDCl_3$, 297 K) CO δ 185.8, 182.7, 181.8 (br, 3C), 177.3, 174.1, 168.1; δ 200.2 (J_{WC} = 13 Hz), 141.6 (*i*-C_6H_5), 138.9 (*i*-C_6H_5), 135.6, 128.2 (2C, *m*-C_6H_5), 128.1 (2C, *m*-C_6H_5), 127.9 (3C, *o*-C_6H_5 and *p*-C_6H_5), 127.6 (2C, *o*-C_6H_5), 126.3 (1C, *p*-C_6H_5), 118.2 (C_5Me_5), 115.6 (*C*H), 114.6, 12.2 (C_5Me_5). Anal. Calcd for $C_{34}H_{26}O_{10}Os_3W$: C, 30.27; H, 1.94. Found: C, 30.09; H, 1.99.

Thermolysis of 2. A toluene solution (40 mL) of **2** (62 mg, 0.044 mmol) was heated at reflux for 3 h, during which time the color of the solution changed from red to yellowish-brown. After the removal of solvent *in vacuo*, the residue was taken up in CH_2Cl_2 and separated by thin-layer chromatography. Development with a 1:1 mixture of CH_2Cl_2 and hexane produced three bands, which were extracted from silica gel to yield 34 mg of orange Cp*W(O)(μ-O)Os$_3$(CCPhCPhCPh)(CO)$_8$ (**5a**, 0.024 mmol, 55%), 11 mg of unreacted complex **2** (0.008 mmol, 18%), and 9 mg of **3a** (0.006 mmol, 14%) in the order of elution. Crystals of **5a** suitable for X-ray diffraction study were obtained by recrystallization from CH_2Cl_2 and methanol at room temperature.

Spectral data for **5a**: MS (FAB, ^{184}W, ^{192}Os) *m*/*z* 1430 (M$^+$); IR (C_6H_{12}) ν(CO) 2091 (vs), 2057 (vs), 2018 (vs), 2005 (vs), 1985 (m), 1969 (s), 1954 (m), 1931 (m), 1925 (m) cm^{-1}; ^{1}H NMR (300 MHz, $CDCl_3$, 297 K) δ 7.62 (d, 2H, J_{HH} = 7.7 Hz), 7.24−6.74 (m, 13H), 2.16 (s, 15H); ^{13}C NMR (75 MHz, $CDCl_3$, 297 K) CO δ 185.3, 184.0, 182.6, 179.5, 179.1, 172.4 (2CO), 171.6. Anal. Calcd for $C_{41}H_{32}Cl_2O_{10}Os_3W$: C, 32.61; H, 2.14. Found: C, 32.66; H, 2.15.

Thermolysis of 3a and 3b. A toluene solution (40 mL) of **3a** (61 mg, 0.043 mmol) was heated at reflux for 1 h. After the removal of solvent *in vacuo*, the residue was taken up in CH_2Cl_2 and separated by thin-layer chromatography (CH_2Cl_2:hexane = 1:1), giving 13 mg of orange **5a** (0.009 mmol, 21%) and 42 mg of the unreacted starting material **3a** (0.029 mmol, 68%). Thermolysis of **3b** in refluxing toluene for 6 h afforded the complex Cp*W(O)(μ-O)Os$_3$(CCPhCHCPh)(CO)$_8$ (**5b**) in 53% yield.

Spectral data for **5b**: MS (FAB, ^{184}W, ^{192}Os) *m*/*z* 1354 (M$^+$); IR (C_6H_{12}) ν(CO) 2092 (vs), 2057 (vs), 2018 (vs), 2005 (vs), 1982 (m), 1969 (s), 1956 (m), 1936 (m) 1930 (w) cm^{-1}; ^{1}H NMR (400 MHz, CD_2Cl_2, 297 K) δ 8.02 (d, 2H, J_{HH} = 8.4 Hz), 7.37−7.30 (m, 4H), 7.18−7.06 (m, 5H), 2.03 (s, 15H); ^{13}C NMR (100 MHz, CD_2Cl_2, 297 K) CO δ 184.6, 184.2, 182.2, 180.5, 179.1, 173.9, 172.4, 171.7. Anal. Calcd for $C_{34}H_{26}O_{10}Os_3W$: C, 30.27; H, 1.94. Found: C, 30.12; H, 2.06.

X-ray Crystallography. The X-ray diffraction measurements for complexes **2a**, **3b**, **4**, and **5a** were carried out on a Nonius CAD-4 diffractometer at room temperature. Lattice parameters were determined from 25 randomly selected high-angle reflections. Three standard reflections were monitored every 3600 s. No significant change in intensities (≤3%) was observed during the course of all data collections. Intensities of the diffraction signals were corrected for Lorentz, polarization, and absorption effects (ψ scans). The structure was solved by using the NRCC-SDP-VAX package. All of the non-hydrogen atoms had anisotropic temperature factors, while the hydrogen atoms were placed at their calculated positions with $U_H = U_C + 0.1$. The crystallographic refinement parameters are summarized in Table 1, while the selected bond distances

(5) (a) Hao, L.; Xiao, J.; Vittal, J. J.; Puddephatt, R. J.; Manojlovic-Muir, L.; Muir, K. W.; Torabi, A. A. *Inorg. Chem.* **1996**, *35*, 658. (b) Graf, I. V. G.; Bacon, J. W.; Consugar, M. B.; Curley, M. E.; Ito, L. N.; Pignolet, L. H. *Inorg. Chem.* **1996**, *35*, 689. (c) Xiao, J.; Hao, L.; Puddephatt, R. J.; Manojlovic-Muir, L.; Muir, K. W. *J. Am. Chem. Soc.* **1995**, *117*, 6316. (d) Hao, L.; Xiao, J.; Vittal, J.; Puddephatt, R. J. *Angew. Chem., Int. Ed. Engl.* **1995**, *34*, 346. (e) Xiao, J.; Puddephatt, R. J. *Coord. Chem. Rev.* **1995**, *143*, 457.

(6) Shiu, C.-H.; Su, C.-J.; Pin, C.-W.; Chi, Y.; Peng, S.-M.; Lee, G.-H. *J. Organomet. Chem.* **1998**, *545−546*, 151.

Table 1. X-ray Structural Data of Complexes 2, 3b, 4, and 5a[a]

compound	**2**	**3b**	**4**	**5a**
formula	$C_{40}H_{30}O_{10}Os_3W$	$C_{34}H_{26}O_{10}Os_3W$	$C_{34}H_{26}O_{10}Os_3W$	$C_{40}H_{30}O_{10}Os_3W{\cdot}CH_2Cl_2$
mol wt	1424.12	1349.01	1349.01	1510.04
cryst syst	triclinic	triclinic	orthorhombic	monoclinic
space group	$P\bar{1}$	$P\bar{1}$	*Pbca*	$P2_1/c$
a (Å)	11.747(2)	10.012(3)	16.904(4)	11.561(3)
b (Å)	11.941(3)	11.861(4)	17.008(3)	15.228(3)
c (Å)	30.970(6)	15.118(4)	24.079(4)	24.813(6)
α (deg)	92.72(2)	84.58(3)		
β (deg)	94.51(2)	85.78(2)		94.18(2)
γ (deg)	113.16(2)	79.58(3)		
volume (Å^3)	3967(1)	1755(1)	6923(2)	4357(2)
Z	4	2	8	4
D_c (g/cm^3)	2.384	2.553	2.589	2.302
F(000)	2587	1214	4854	2756
2*θ* (max), deg	50	50.0	50.0	50.0
h, *k*, *l* ranges	−13 to 12, 0 to 14, −36 to 36	−11 to 11, 0 to 14, −17 to 17	0 to 20, 0 to 20, 0 to 28	−13 to 13, 0 to 18, 0 to 29
cryst size, mm	0.15 × 0.25 × 0.35	0.05 × 0.25 × 0.40	0.05 × 0.30 × 0.50	0.10 × 0.50 × 0.50
μ(Mo Kα), cm^{-1}	155.51	142.34	144.29	115.96
transmission: max, min	1.000, 0.459	1.000, 0.347	1.000, 0.216	0.115, 0.014
no. of data in refinement	9849 with $I \geq 2\sigma(I)$	4954 with $I \geq 2\sigma(I)$	4137 with $I \geq 2\sigma(I)$	4851 with $I \geq 2\sigma(I)$
no. of atoms and params	170, 974	74, 434	82, 470	89, 515
weight modifer, *g*	0.00007	0.00003	0.0001	0.0001
max Δ/*σ* ratio	0.012	0.002	0.045	0.02
R_F; R_w	0.029; 0.029	0.032; 0.032	0.044; 0.044	0.047; 0.042
GOF	1.28	1.79	1.81	1.69
D-map, max/min, e/Å^3	1.39/−0.95	1.94/−1.89	2.40/−1.82	2.01/−1.65

[a] Features common to all determinations: Nonius CAD-4 diffractometer, λ(Mo Kα) = 0.7107 Å. Minimized function: $\sum(w|F_o - F_c|^2)$. Weighting scheme: $w^{-1} = \sigma^2(F_o) + |g|F_o^2$. GOF = $[\sum w|F_o - F_c|^2/(N_o - N_v)]^{1/2}$ (N_o = number of observations; N_v = number of variables).

and angles of each individual complex are presented in Tables 2−5, respectively.

Finally, it is important to note that the C(20), C(21), C(23), and C(24) carbon atoms of complex **4** occupy two alternative sites, each with 50% occupancy. The phenyl group associated with these four carbon atoms shares the ordered carbon atoms, C(19) and C(22), which are located at the ipso and the para position (Figure 1S of the Supporting Information). Only one set of these disordered carbon atoms is shown for clarity.

Results

Treatment of the acetylide cluster Cp*$WOs_3(\mu\text{-}O)_2$-$(CCPh)(CO)_9$ (**1**) with diphenylacetylene at 100 °C affords two complexes Cp*$W(O)Os_3(\mu\text{-}O)(CCPh)(PhC_2$-$Ph)(CO)_8$ (**2**) and Cp*$W(O)Os_3(\mu\text{-}O)(CCPhCPhCPh)(CO)_8$ (**3a**) in moderate yields. The reaction of **1** with phenylacetylene at 90 °C in toluene gives rise to the isolation of Cp*$W(O)Os_3(\mu\text{-}O)(CCPhCHCPh)(CO)_8$ (**3b**), together with small amounts of Cp*$W(O)Os_3(\mu\text{-}O)(CCPhCCHPh)$-$(CO)_8$ (**4**). These new cluster complexes were separated by thin-layer chromatography and recrystallization. The FAB mass analysis suggests that each of them was produced by incorporation of one alkyne molecule induced by removal of one CO ligand, showing a parent ion (M^+) at $m/z = 1430$ for **2** and **3a** and $m/z = 1354$ for **3b** and **4**. Consistent with the mass analysis, the ^{13}C NMR spectra of ^{13}CO-enriched samples show the presence of eight Os−CO ligands for each complex. Moreover, the IR spectrum of **3b** exhibits a *ν*(CO) pattern which is analogous to that of **3a**, suggesting that they possess an identical cluster core arrangement. Single-crystal X-ray analyses of complexes **2**, **3b**, and **4** were carried out to reveal their molecular structures.

Complex **2** crystallizes in a triclinic space group with two crystallographically independent but structurally similar molecules in the unit cell. Its molecular geometry is shown in Figure 1 together with the atomic-numbering scheme, while selective bond angles and

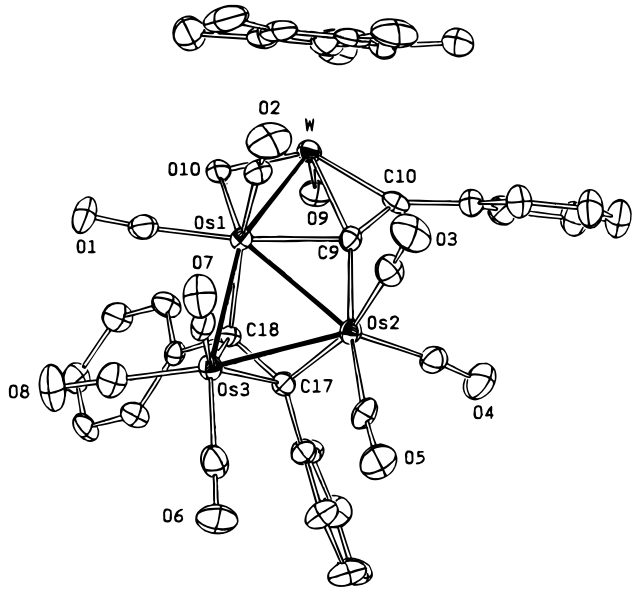

Figure 1. Molecular structure and atomic-labeling scheme of Cp*$W(O)Os_3(\mu\text{-}O)(CCPh)(PhC_2Ph(CO)_8$ (**2**), with thermal ellipsoids shown at the 30% probability level.

Table 2. Selected Bond Distances (Å) and Bond Angles (deg) of 2 (esd in Parentheses)

W−Os(1)	2.994(1)	Os(1)−Os(2)	2.7724(7)
Os(1)−Os(3)	2.6878(8)	Os(2)−Os(3)	2.750(1)
W−O(9)	1.697(6)	W−O(10)	1.839(6)
Os(1)−O(10)	2.060(6)	W−C(9)	2.422(9)
W−C(10)	2.093(9)	Os(1)−C(9)	2.129(8)
Os(2)−C(9)	2.129(9)	C(9)−C(10)	1.32(1)
Os(2)−C(17)	2.124(9)	Os(3)−C(17)	2.287(8)
Os(1)−C(18)	2.122(8)	Os(3)−C(18)	2.290(8)
C(17)−C(18)	1.39(1)		
∠W−O(10)−Os(1)	100.2(3)	∠O(9)−W−O(10)	104.9(3)
∠Os(2)−C(9)−C(10)	138.2(7)	∠C(9)−C(10)−C(11)	133.7(9)

distances are given in Table 2. The cluster skeleton consists of a spiked-triangular arrangement with three

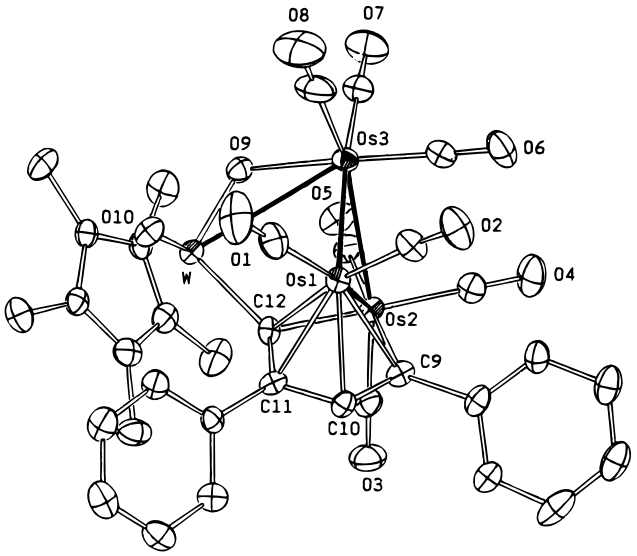

Figure 2. Molecular structure and atomic-labeling scheme of $Cp^*W(O)Os_3(\mu\text{-}O)(CCPhCPhCPh)(CO)_8$ (**3b**), with thermal ellipsoids shown at the 30% probability level.

osmium atoms constituting the central metal triangle, on which the $(C_5Me_5)W(O)_2$ fragment is coordinated to the Os(1) atom with a slightly elongated W−Os distance (2.994(1) Å). The Os(2) and Os(3) atoms each carry three mutually orthogonal, terminal CO ligands, while the osmium atom Os(1) possesses only two CO ligands as the third coordination site is occupied by the bridging oxo ligand. The diphenylacetylene ligand is attached to the Os_3 triangle via a $2\sigma + \pi$ mode, which is typical for osmium alkyne cluster complexes reported in the literature.[7] The acetylide ligand interacts with both the W atom and the Os(1)−Os(2) edge, adopting a novel μ_3-bonding mode which is quite similar to that observed in the structurally characterized, acetylide cluster $Cp^*W(O)Re_2(CCR)(CO)_8$, R = CMe=CH_2.[8] However, the W−C(10) distance in **2** (2.093(9) Å) is substantially longer than the corresponding W−C distance observed in the WRe_2 cluster (2.012(9) Å), suggesting the absence of any W=C multiple bonding character. The weakening of the W−C bond is presumably attributed to the competing, strong W=O bonding exerted by the bridging oxo ligand O(10), which, in principle, reduces the bonding between the tungsten and carbon atom C(10) at the trans position. Likewise, the long W−C(9) distance (2.422(9) Å) also reflects the poor capability of the acetylide β-carbon to compete with the *trans*-oxo ligand O(11) for bonding to the tungsten atom.

The molecular structure of **3b** is shown in Figure 2, and bond distances are given in Table 3. Similar to that of **2**, the cluster framework shows a spiked-triangular arrangement comoposed of one $Cp^*W(O)_2$ unit and one $Os(CO)_2$ and two $Os(CO)_3$ fragments, but significant differences are also noticed. For example, the $Cp^*W(O)_2$ fragment of **3b** resides at a location perpendicular to the osmium triangle but not parallel to the triosmium plane as observed in complex **2**. In addition, one oxo ligand adopts a terminal bonding mode, while the second oxo ligand spans the W−Os(3) edge (3.298(1) Å)

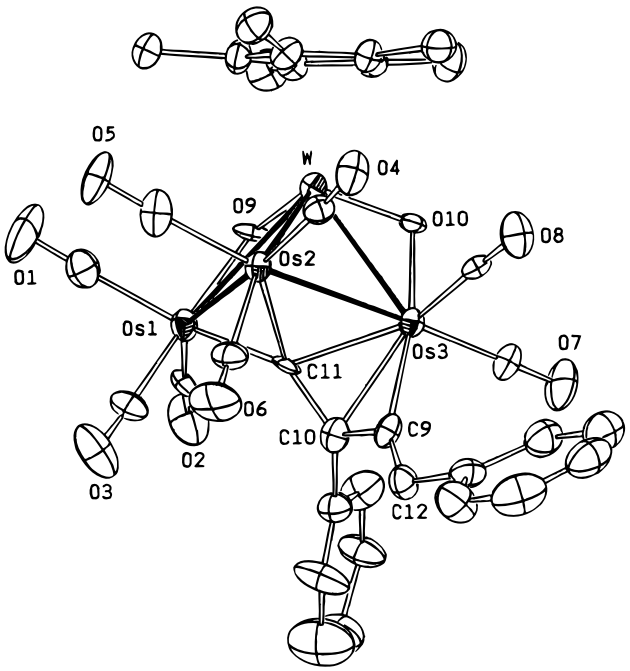

Figure 3. Molecular structure and atomic-labeling scheme of $Cp^*W(O)Os_3(\mu\text{-}O)(CCPhCCHPh)(CO)_8$ (**4**), with thermal ellipsoids shown at the 30% probability level.

Table 3. Selected Bond Distances (Å) and Bond Angles (deg) of 3b (esd in Parentheses)

W···Os(1)	3.427(1)	W···Os(2)	3.513(1)
W−Os(3)	3.298(1)	Os(1)−Os(2)	2.7242(9)
Os(1)−Os(3)	2.773(1)	Os(2)−Os(3)	2.881(1)
W−O(9)	1.799(9)	W−O(10)	1.725(6)
Os(3)−O(9)	2.145(7)	W−C(12)	2.072(9)
Os(1)−C(12)	2.226(9)	Os(2)−C(12)	2.192(9)
Os(1)−C(11)	2.29(1)	Os(1)−C(10)	2.263(9)
Os(1)−C(9)	2.232(9)	Os(2)−C(9)	2.149(9)
C(9)−C(10)	1.38(1)	C(10)−C(11)	1.40(1)
C(11)−C(12)	1.42(1)		
∠W−O(9)−Os(3)		113.2(3)	

and connects to the Os(3) atom at a site opposite to the axial CO(6) ligand. The tungsten atom connects to the C_α atom of the acetylide ligand, while the acetylide is linked to the phenylacetylene fragment in a head-to-tail fashion, forming a fused C_4Ph_3 fragment. The C_4 backbone surrounds the Os(1)−Os(2) edge such that its local arrangement exhibits a pattern resembling that of the metallacyclopentadienyl fragment,[9] for which the Os(2)−C(9)−C(10)−C(11)−C(12) pentagon is coordinated to the Os(1) atom via two alkenic π-interactions and the Os(1)−Os(2) bond, and to the third metal atom via the W−C(12) bond. Thus, the formation of **3b** is induced by a coupling of the acetylide and alkyne ligands.

Figure 3 illustrates a molecular drawing of **4**, while selected bond lengths and angles are summarized in Table 4. The ORTEP diagram displays a butterfly metal arrangement in which the tungsten atom occupies one of the hinge sites, while the oxo ligands are each coordinated to the osmium atoms Os(1) and Os(3) at the wingtip positions, in a manner similar to that observed

(7) (a) Sappa, E.; Tiripicchio, A.; Braunstein, P. *Chem. Rev.* **1983**, *83*, 203. (b) Sappa, E. *J. Cluster Sci.* **1994**, *5*, 211.

(8) Chi, Y.; Wu, H.-L.; Chen, C.-C.; Su, C.-J.; Peng, S.-M.; Lee, G.-H. *Organometallics* **1997**, *16*, 2443.

(9) (a) Deeming, A. J. *Adv. Organomet. Chem.* **1986**, *26*, 1. (b) Ferraris, G.; Gervasio, G. *J. Chem. Soc., Dalton Trans.* **1972**, 1057. (c) Chi, Y.; Wu, H.-L.; Peng, S.-M.; Lee, G.-H. *J. Chem. Soc., Dalton Trans.* **1997**, 1931.

Table 4. Selected Bond Distances (Å) and Bond Angles (deg) of 4 (esd in Parentheses)

W−Os(1)	3.084(1)	W−Os(2)	2.724(1)
W−Os(3)	2.998(1)	Os(1)···Os(3)	3.979(1)
Os(1)−Os(2)	2.816(1)	Os(2)−Os(3)	2.862(1)
W−O(9)	1.76(1)	W−O(10)	1.77(1)
Os(1)−O(9)	2.18(1)	Os(3)−O(10)	2.22(2)
Os(1)−C(11)	2.04(2)	Os(2)−C(11)	2.17(2)
Os(3)−C(11)	2.22(2)	Os(3)−C(10)	2.23(2)
Os(3)−C(9)	2.03(2)	C(10)−C(11)	1.39(2)
C(9)−C(10)	1.45(2)	C(9)−C(12)	1.32(2)
∠W−O(9)−Os(1)	102.3(5)	∠W−O(10)−Os(3)	97.0(4)
∠C(9)−C(12)−C(13)	126(2)		

in the dioxo carbonyl cluster $CpWOs_3(\mu\text{-}O)_2(\mu\text{-}H)(CO)_9$ and complex **1**.[3a,7a] The resulting W−Os vectors (W−Os(1) = 3.084(1) Å and W−Os(3) = 2.998(1) Å) are significantly longer than the unbridged W−Os(2) edge (2.724(1) Å), which is attributable to the relatively smaller atomic radius for the tungsten atom in the higher oxidation state. The Os(1)−Os(3) distance (3.979(1) Å) is clearly out of the range expected for a significant Os−Os single bond. The C_4 fragment, which is produced by the coupling of phenylacetylide and phenylacetylene ligands, is arranged in a head-to-tail fashion. The C_α carbon atom C(11) of the acetylide shows a strong bonding interaction to the Os(1) atom (2.04(2) Å) with respect to other osmium atoms (Os(2)−C(11) = 2.17(2) Å and Os(3)−C(11) = 2.22(2) Å), while the C_β carbon atom C(10) is linked to only one Os atom Os(3) and the carbon atom C(9). Interestingly, the hydrogen atom of the phenylacetylene is no longer attached to the C_α atom C(9) but has migrated to the adjacent C_β atom C(12), producing an enyl fragment. Thus, this observed structural feature supports the occurrence of a 1,2-hydrogen migration on phenylacetylide during the formation of **4**.

In attempts to explore the chemical and structural relationship between these cluster complexes, we have investigated the reactivities of **2**, **3a**, and **3b**. Thus, heating a solution of **2** in refluxing toluene (1 h) affords a mixture of unreacted **2** (18%) and complex **3a** (14%) and a yellow complex $Cp^*W(O)Os_3(\mu\text{-}O)(CCPhCPhCPh)(CO)_8$ (**5a**) in 55% yield. Furthermore, thermolysis of **3a** (110 °C, 1 h) gives rise to the formation of **5a** in good yield, while treatment of **3b** in refluxing toluene solution for 6 h also leads to the generation of **5b** in 53% yield. On the basis of the above results, it is likely that complex **2** first converts to complex **3**, which then gives the thermodynamic complex **5** as the final product.

An X-ray diffraction study of **5a** was carried out to verify its identity. As indicated in Figure 4 and Table 5, the core structure consists of a bent-chain or an open-planar cluster[10] in which the metal atoms are connected by three metal−metal bonds. The Os(1)−Os(2) and Os(2)−Os(3) bond distances are 2.909(1) and 2.786(1) Å, respectively, much longer than the third W−Os(3) distance (2.632(1) Å), which is characteristic of bonding between a high oxidation state tungsten atom and a osmium carbonyl fragment. The bridging oxo ligand O(9) is located between the W and Os(1) atoms with distances W−Os(1) = 3.408(1) Å, W−O(9) = 1.803(9) Å, and Os(1)−O(9) = 2.10(1) Å. Again, this bridging interaction results in an increase in the bridged W═O distance compared to that of the terminal oxo ligand O(10), W−O(10) = 1.67(1) Å. In addition, the metallacyclopentadienyl ligand, which is now associated with the osmium carbonyl fragments, suggests the existence of an intramolecular interchange between the $Cp^*W(O)_2$ fragment and one of the $Os(CO)_3$ units during the conversion from **3** to **5**.

(10) Two examples of these types of compounds have been reported, see: Adams, R. D.; Horvath, I. T.; Natarajan, K. *Organometallics* **1984**, *3*, 1540.

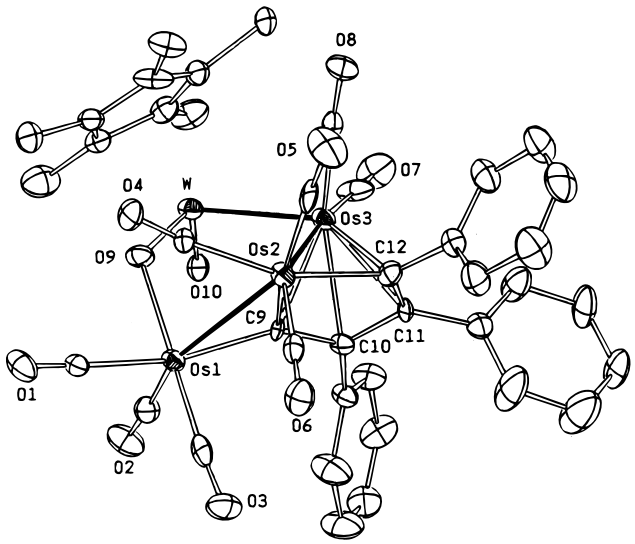

Figure 4. Molecular structure and atomic-labeling scheme of $Cp^*W(O)(\mu\text{-}O)Os_3(CCPhCPhCPh)(CO)_8$ (**5a**), with thermal ellipsoids shown at the 30% probability level.

Table 5. Selected Bond Distances (Å) and Bond Angles (deg) of 5a (esd in Parentheses)

W···Os(1)	3.408(1)	W···Os(2)	4.038(1)
W−Os(3)	2.632(1)	Os(1)−Os(2)	2.909(1)
Os(2)−Os(3)	2.786(1)	W−O(9)	1.803(9)
Os(1)−O(9)	2.10(1)	Os(1)−C(9)	2.01(1)
W−O(10)	1.67(1)	Os(2)−C(9)	2.10(1)
Os(3)−C(9)	2.26(1)	Os(3)−C(10)	2.29(1)
Os(3)−C(11)	2.28(2)	Os(3)−C(12)	2.33(2)
Os(2)−C(12)	2.10(2)	C(9)−C(10)	1.42(2)
C(10)−C(11)	1.43(2)	C(11)−C(12)	1.42(2)
∠Os(1)−Os(2)−Os(3)	86.05(3)	∠Os(2)−Os(3)−W	96.34(4)
∠O(9)−W−O(10)	106.6(5)	∠Os(3)−W−O(9)	99.8(4)
∠O(3)−W−O(10)	100.0(4)	∠O(9)−W−O(10)	121.7(6)

Discussion

The reaction of **1** with diphenylacetylene proceeds rapidly at elevated temperature to afford the cluster compounds **2** and **3a** in moderate yields. Compound **2** appears as the kinetic product for this reaction as it contains discrete acetylide and alkyne ligands. The reaction presumably occurs by direct coordination of alkyne to the triosmium framework, where the required coordinative unsaturation is provided by the elimination of a CO ligand and transfer of a bridging oxo ligand to the terminal mode (Scheme 2). The coordination of alkynes to triosmium frameworks is well-documented. Representative examples involve the addition of alkynes to the unsaturated dihydride cluster $H_2Os_3(CO)_{10}$ or other triosmium complexes activated by addition of Me_3NO.[11] All of these product complexes possess a ligated alkyne linked to the triosmium face via the $\mu_3\text{-}\eta^2$-mode.

After the formation of **2**, rearrangement to the relatively more stable complexes **3a** and **5a** can be easily

Scheme 2

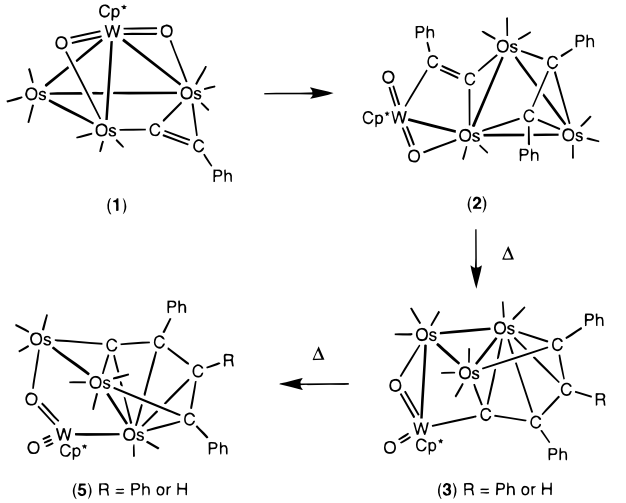

Scheme 3

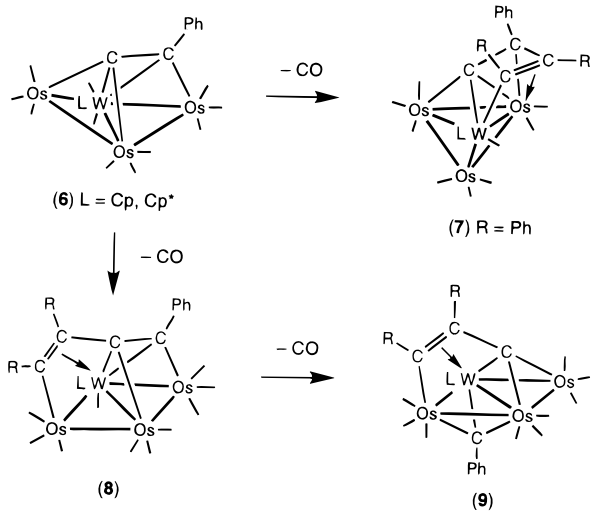

Scheme 4

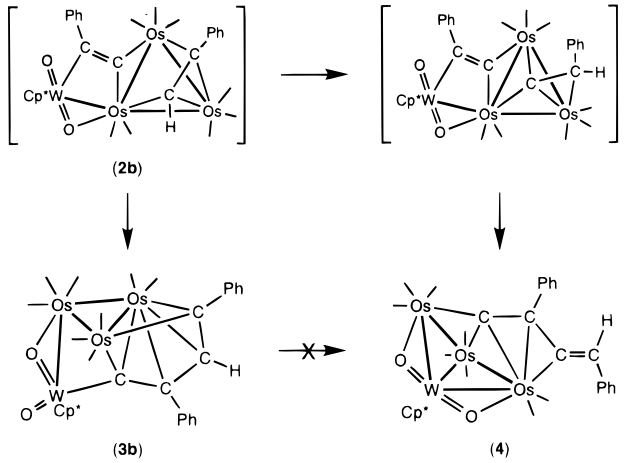

achieved by extensive heating in solution. This reaction involves the cluster-assisted coupling of acetylide and alkyne, leading to the formation of the metallacyclopentadienyl fragment, and then skeletal isomerization involving rotation of the $Cp^*W(O)_2-Os(CO)_3$ unit against the metallacyclopentadienyl fragment. In principle, the first reaction is conceptually similar to the coupling of acetylide and alkynes observed in other cluster systems.[12]

However, because of the high oxidation state $Cp^*W(O)_2$ unit introduced, the reactivity pattern of **1** with alkynes has changed completely. This is best illustrated by a similar alkyne−acetylide coupling reaction of the related WOs_3 acetylide complex **6** which bears a low oxidation state $W(CO)_2$ fragment.[13] As indicated in Scheme 3, two coupling products **7** and **8** were isolated following the elimination of a CO ligand from the tungsten atom. The surprising product of this reaction is compound **9**, which is generated by the removal of the second CO ligand from the tungsten atom, together with the cleavage of the C−C bond. It appears to us that the W═O multiple bonds in **1** are simply too strong for that to be realized.

On the other hand, for the reaction of **1** with a terminal alkyne, the analogous complex **2b** was not observed during the reaction but we isolated two related acetylide−acetylene coupling products **3b** and **4** in moderate yields. On the basis of our previous discussion, there is no doubt that complex **3b** is produced through the initial formation of **2b** as an intermediate (Scheme 4). In addition, as the second complex **4** involves a CCHPh terminus on the C_4 fragment, it is possible that the coordinated phenylacetylene in **2b** would undergo a rapid 1,2-hydrogen migration to afford a transient vinylidene fragment, which then couples with the acetylide ligand to afford the C_4 fragment. This observation is fully compatible with the facile acetylide-to-vinylidene conversion on the trinuclear cluster system and the higher nuclearity cluster compounds.[14] An alternative route involves the sequential alkyne coordination, acetylide−alkyne coupling, and 1,2-hydrogen migration on the coupled C_4 fragment. However, this possibility is eliminated as thermolysis of **3b** failed to yield even a trace amount of **4** but afforded a second metallacyclopentadienyl cluster compound **5b**, of which the structure is identical to the diphenylacetylene-substituted complex **5a** prepared by heating of **3a** under similar conditions (Scheme 2).

Finally, variation of the bonding for the O═W═O→Os motif in the clusters **2**, **3**, and **5** is also noteworthy. As revealed in Chart 1, the W−Os distances observed in complexes **2** and **4** is in the range 2.994(1)−3.084(1) Å, which are normal bond distances and are closely related to those observed in the WOs_3 clusters bearing one bridging oxo ligand,[15] suggesting the existence of W−Os

(11) (a) Bracker-Novak, J.; Hajela, S.; Lord, M.; Zhang, M.; Roseberg, E.; Goberto, R.; Milone, L.; Osella, D. *Organometallics* **1990**, *9*, 1379. (b) Deeming, A. J.; Senior, A. M. *J. Organomet. Chem*. **1992**, *439*, 177. (c) Adams, R. D.; Chen, G.; Qu, X.; Wu, W.; Yamamoto, J. H. *Organometallics* **1993**, *12*, 3029. (d) Deeming, A. J.; Felix, M. S. B.; Nuel, D. *Inorg. Chim. Acta* **1993**, *213*, 3.

(12) (a) Sappa, E.; Pasquinelli, G.; Tiripicchio, A.; Camellini, M. T. *J. Chem. Soc., Dalton Trans*. **1989**, 601. (b) Chi, Y.; Huttner, G.; Imhof, W. *J. Organomet. Chem*. **1990**, *384*, 93. (c) Chi, Y.; Wu, C.-H.; Peng, S.-M.; Lee, G.-H. *Organometallics* **1990**, *9*, 2305. (d) Chi, Y.; Shu, H.-Y.; Peng, S.-M.; Lee, G.-H. *J. Chem. Soc., Chem. Commun*. **1991**, 1023. (e) Corrigan, J. F.; Doherty, S.; Taylor, N. J.; Carty, A. J. *Organometallics* **1992**, *11*, 3160.

(13) (a) Chi, Y.; Hsu, S.-F.; Peng, S.-M.; Lee, G.-H. *J. Chem. Soc., Chem. Commun*. **1991**, 1019. (b) Chi, Y. *J. Chin. Chem. Soc.* **1992**, *39*, 591. (b) Chi, Y.; Lin, R.-C.; Chen, C.-C.; Peng, S.-M.; Lee, G.-H. *J. Organomet. Chem*. **1992**, *439*, 347.

(14) (a) Albiez, T.; Bernhardt, W.; Schnering, C. V.; Roland, E.; Bantel, H.; Vahrenkamp, H. *Chem. Ber*. **1987**, *120*, 141. (b) Albiez, T.; Bantel, H.; Vahrenkamp, H. *Chem. Ber*. **1990**, *123*, 1805. (c) Bruce, M. I. *Chem. Rev*. **1991**, *91*, 197.

Chart 1

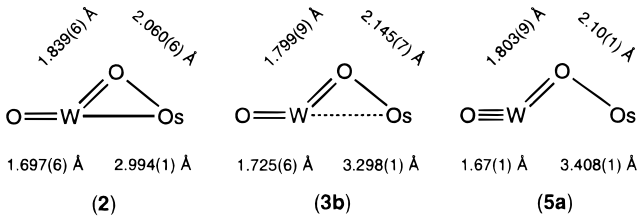

single-bond interactions. However, the corresponding W−Os distance increases to 3.298(1) Å for **3b** and to 3.408(1) Å for **5a**, indicating that the metal atoms in these two complexes are either weakly bonded or completely nonbonded. The nature of bond elongation is not clear at present, but it could be due to the presence of the C_4 fragment which serves as an interlocking device to prevent the tungsten and the osmium metal atoms to bond to each other. In addition, if the terminal and the bridging oxo ligand were considered as a two-electron and four-electron donor, respectively, electron counting would give a total of 64 cluster valence electrons for all three cluster complexes **2**, **3**, and **5**. The first two complexes **2** and **3** are electron precise as they contain four M−M bonds arranged in the spiked-triangular geometry. On the contrary, complex **5**, which possess only three direct M−M bonds, is deemed to be electron deficient or unsaturated according to the predictions of the 18-electron rule.

However, the chemical reactivity of **5** contradicts with this prediction as these compounds failed to react with carbon monoxide (1 atm, 100 °C) to yield the CO addition product but afforded a fragmentation product with formula $Cp^*W(O)_2Os_2(CCPhCRCPh)(CO)_6$, R = Ph or H, under pressurized CO and extensive heating. Therefore, it seems that complexes **5** exhibit the characteristic feature of an electron-precise, bent-chain complex containing 66-cluster valence electrons. One possible explanation is that the terminal oxo ligand now serves as a four-electron donor rather than the two-electron donor we proposed earlier. Thus, the additional dative π-bonding from the terminal oxo ligand to the tungsten metal atom compensates for the electron deficiency caused by the cleavage of the W−Os bond. In fact, the relatively short W−O(terminal) distance observed for **5a** supports the existence of a strong W≡O multiple bond interaction.[16]

Acknowledgment. We thank the National Science Council of the Republic of China for financial support (Grant No. NSC 86-2113-M007-035).

Supporting Information Available: Tables of atomic coordinates and anisotropic thermal parameters for complexes **2**, **3b**, **4**, and **5a** and ORTEP diagram of **4** (26 pages). Ordering information is given on any current masthead page.

OM980025V

(15) (a) Churchill, M. R.; Bueno, C.; Park, J. T.; Shapley, J. R. *Inorg. Chem*. **1984**, *23*, 1017. (b) Chi, Y.; Shapley, J. R.; Churchill, M. R.; Li, Y.-J. *Inorg. Chem*. **1986**, *25*, 4165. (c) Chi, Y.; Shapley, J. R.; Ziller, J. W.; Churchill, M. R. *Organometallics* **1987**, *6*, 301. (d) Park, J.-T.; Chung, M.-K.; Chun, K. M.; Yun, S. S.; Kim, S. *Organometallics* **1992**, *11*, 3313. (e) Gong, J.-H.; Chen, C.-C.; Chi, Y.; Wang, S.-L.; Liao, F.-L. *J. Chem. Soc., Dalton Trans.* **1993**, 1829. (f) Park, J. T.; Chi, Y.; Shapley, J. R.; Churchill, M. R.; Ziller, J. W. *Organometallics* **1994**, *13*, 813.

(16) Su, C.-J.; Su, P.-C.; Chi, Y.; Peng, S.-M.; Lee, G.-H. *J. Am. Chem. Soc.* **1996**, *118*, 3289.